View metadata, citation and similar papers at core.ac.uk

brought to you by CORE

provided by City Research Online

City Research Online

City, University of London Institutional Repository

Citation: Giaralis, A. & Taflanidis, A. A. (2016). Robust reliability-based design of seismically excited tuned mass-damper-inerter (TMDI) equipped MDOF structures with uncertain properties. Paper presented at the 6th European Conference on Structural Control - EACS2016, 11-13 Jul 2016, Sheffield, England.

This is the accepted version of the paper.

This version of the publication may differ from the final published version.

Permanent repository link: http://openaccess.city.ac.uk/19269/

Link to published version:

Copyright and reuse: City Research Online aims to make research outputs of City, University of London available to a wider audience. Copyright and Moral Rights remain with the author(s) and/or copyright holders. URLs from City Research Online may be freely distributed and linked to.

City Research Online: http://openaccess.city.ac.uk/ publications@city.ac.uk

Robust reliability-based design of seismically excited tuned mass-damper-inerter (TMDI) equipped MDOF structures with uncertain properties

Agathoklis Giaralis[1]*, Alexandros Taflanidis[2]

[1]*Dept. of Civil Eng., City University London, London, UK*

[2]*Dept. of Civil and Environmental Eng. and Earth Sciences, University of Notre Dame, Notre Dame, IN,USA*

ABSTRACT

This paper considers a reliability-based approach for the optimal design of the tuned mass-damper-inerter (TMDI) in linear building frames with uncertain structural properties subject to seismic excitations defined as stationary colored random processes with uncertain parameters. The TMDI is a recently introduced generalization of the classical linear passive tuned mass-damper (TMD) comprising an additional mass attached to the primary structure whose oscillations are to be suppressed via a linear spring and dashpot in parallel. The TMDI benefits from the mass amplification property, the so-called inertance, of an inerter device that links the additional mass to a different floor from the one it is attached to which improves the vibration suppression capabilities of the TMD. Herein, the structural seismic performance is quantified through the probability of occurrence of different failure modes, related to the floor acceleration, the inter-storey drifts, and the attached mass displacement exceeding acceptable thresholds. The overall design objective is taken as a linear combination of these probabilities whereas the TMDI linear spring constant, viscous damping constant, and inertance properties are taken as the design variables. The parametric structural and excitation uncertainty is efficiently addressed through a two-stage approach combining a Taylor series approximation and Monte Carlo simulation. Numerical data for a 10-storey shear frame structure equipped with a TMDI with different values of attached mass and arranged in 8 different topologies are furnished indicating the enhanced performance of the TMDI over the classical TMD for relatively small attached masses. The reported numerical results evidence that the performance of optimally designed TMDIs is less affected by the parametric uncertainties as the total inertia TMDI properties (attached mass and inertance) increases, indicating that the inclusion of the inerter leads to more robust passive vibration control.

Keywords: *Tuned mass damper, inerter, reliability, model uncertainty, stochastic optimization, earthquake*

1 INTRODUCTION

Over the past several decades, the concept of the passive tuned mass-damper (TMD) has been extensively considered to mitigate earthquake-induced vibrations in building structures (e.g., [1-4]). The TMD comprises a mass attached towards the top of the structure whose vibration motion is to be controlled (primary structure) via optimally designed/"tuned" linear spring and dashpot elements. Although closed-form expressions for optimum TMD properties do exist (e.g., [5]), numerical optimization routines are commonly employed for TMD design. No matter what performance criteria are adopted in this design, it is widely recognized that the TMD effectiveness for the seismic protection of structures depends heavily on its inertia properties [2-4]. Practically speaking, the larger the attached TMD mass that can be accommodated, subject to structural design and architectural constraints, the more effective the TMD will be to suppress the primary structure oscillations and the more robust it will be in terms of detuning effects. The latter is a well-

[1] Senior Lecturer, agathoklis.giaralis.1@city.ac.uk

[2] Associate Professor, ataflani@nd.edu

* Corresponding author

recognized in the literature drawback of the TMD related to deviations of the dynamic properties of the primary structure and/or of the properties of the input excitation assumed in the TMD design which reduce the effectiveness of the TMD to mitigate vibrations.

To this end, recently, a generalization of the classical TMD has been proposed by Marian and Giaralis [6,7] incorporating an "inerter" device: the tuned mass-damper-inerter (TMDI). The inerter is a two-terminal mechanical device developing a resisting force proportional to the relative acceleration of its terminals [8]. The underlying constant of proportionality ("inertance") can be orders of magnitude larger than the physical mass of the device. In this regard, it was shown analytically and numerically that optimally designed TMDI, treating the attached mass and inertance as fixed quantities, outperforms the classical TMD in terms of relative displacement variance of linear primary structures under broad-band and narrow-band stochastic base excitations by exploiting the "mass amplification" property of the inerter [8]. Moreover, Giaralis and Taflanidis [9] employed a reliability-based optimum design approach to study the effectiveness of several different TMDI topologies for vibration suppression in linear multi-storey building structures excited by stochastic seismic excitation, while Giaralis and Marian [10] demonstrated that the TMDI can achieve the same seismic structural performance level for significantly smaller attached mass compared to the classical TMD.

In all the aforementioned studies on the optimum TMDI design, both the primary structure and the parametrically defined stochastic excitation were assumed to be deterministically known. Herein, the influence of the uncertainty in both the structural properties of the primary structure and frequency content of the seismic excitation to the seismic performance of TMDI equipped multi-storey buildings is examined. To this aim, a reliability-based optimum design approach is adopted in which the structural seismic performance is quantified through the probability of occurrence of different failure modes, related to the floor acceleration, the inter-storey drifts, and the attached mass displacement exceeding acceptable thresholds. The seismic excitation is modelled as a stationary colored Gaussian stochastic process with uncertain properties and, therefore, the above probability corresponds to the first-passage failure probability associated with different failure modes. The overall design objective is taken as a linear combination of these probabilities: this is a different objective function than the one considered in [9] and in previous relevant studies in the literature (e.g. [11]). It is purposely tailored to conform to the current trends in performance based earthquake engineering applications [12]. The TMDI linear spring constant, viscous damping constant, and inertance properties are taken as the design variables. The parametric structural and excitation uncertainty is efficiently addressed through a two-stage approach combining a Taylor series expansion approximation and Monte Carlo simulation. Numerical data pertaining to a 10-storey shear frame structure equipped with a TMDI with different values of attached mass and arranged in 8 different topologies are furnished to assess the seismic performance of TMDI equipped multi-storey structures and to quantify the robustness of optimally designed TMDIs vis-à-vis the classical TMD to structural and seismic input uncertainty.

The governing equations of motion for TMDI equipped linear multi-degree-of-freedom structures are reviewed in the next section, followed (Section 3) by a description of the adopted reliability-based optimal design approach. Section 4 presents a case study for a 10-storey TMDI equipped building frame exposed to stochastic seismic excitation. Concluding remarks are finally summarized in Section 5.

2 THE TUNED MASS-DAMPER-INERTER (TMDI) SYSTEM FOR MULTI-STOREY FRAME BUILDING STRUCTURES

2.1 The ideal linear inerter

Conceptually introduced by Smith [8], the ideal inerter is a linear two terminal device of negligible mass/weight developing an internal (resisting) force proportional to the relative

acceleration of its terminals which are free to move independently. As an example, the internal force of the inerter shown in the inlet of Fig. 1 is given by

$$F = b(\ddot{x}_d - \ddot{x}_{i_b}), \tag{1}$$

where x_d and x_{ib} are the displacement coordinates of the inerter terminals and, hereafter, a dot over a symbol signifies time differentiation. In the above equation, the constant of proportionality b is the so-called inertance and has mass units. Importantly, the physical mass of actual inerter devices can be two or more orders of magnitude lower than b. This has been experimentally validated by testing several flywheel-based prototyped inerter devices incorporating rack-and-pinion or ball-screw mechanisms to transform the translational kinetic energy into rotational kinetic energy stored in a lightweight rotating disk [13]. More recently, hydraulic and fluid based inerters achieving inertance values b that are almost independent of the physical device mass were also been prototyped and tested [14,15]. In this regard, the ideal inerter can be construed as an inertial amplification device, since by "grounding" any one of its terminals, the device acts as a "weightless" mass b developing a resisting force proportional to the acceleration of the ungrounded terminal [8]. This observation motivated the consideration of the tuned mass-damper-inerter, reviewed in the next sub-section, to improve the vibration suppression capabilities of the classical tuned mass-damper for the same attached mass (and thus weight) by exploiting the inertial amplification property of the inerter [6,7].

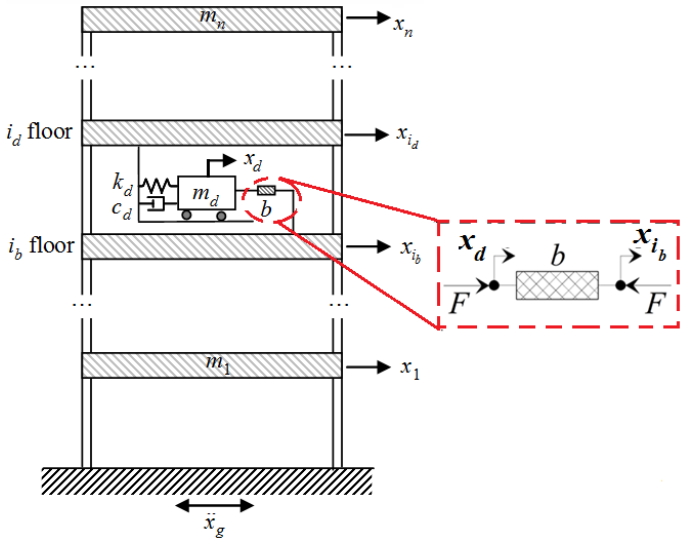

Figure 1- Tuned mass-damper-inerter (TMDI) equipped seismically excited n-storey frame.

2.2 Equations of motion of TMDI equipped multi degree of freedom (MDOF) structures

Consider the planar n-storey frame building, shown in Fig. 1, whose oscillatory motion due to a ground acceleration $\ddot{x}_g$ is to be suppressed (primary structure). The TMDI consists of a classical linear passive tuned mass-damper (TMD) located at the i_d-th floor of the primary structure comprising a mass m_d attached to the structure via a linear spring of stiffness k_d and a linear dashpot of damping coefficient c_d. The TMD mass is linked to the i_b-th floor by an inerter device with inertance b. This is a more general configuration than the one considered in [6,7] where the TMD was located at the top floor and the inerter was linking the attached mass to the penultimate floor, and it allows the evaluation of different topologies for the TMDI implementation. The equations of motion are established by means of *location* and *connectivity* vectors as detailed below.

Let $\mathbf{x}_s \in \mathbb{R}^n$ be the vector collecting the floor displacements of the primary structure relative to the ground motion. Denote by $\mathbf{R}_d \in \mathbb{R}^n$ the *TMD location* vector specifying the floor the TMD is attached to (i.e., vector of zeros with a single one in its i_d entry), and by $\mathbf{R}_b \in \mathbb{R}^n$ the *inerter location* vector specifying the floor the inerter is connected to (i.e., vector of zeros with a single one

in its i_b entry). Further, let $y \in \mathbb{R}$ be the displacement of the TMD mass relative to the i_d floor (i.e., $y = x_d - x_{i_d}$) and define the *connectivity* vector by $\mathbf{R}_c$=$\mathbf{R}_d$-$\mathbf{R}_b$. Then, the resisting force F developing within the inerter is equal to $b(\mathbf{R}_c\ddot{\mathbf{x}}_\mathbf{s} + \ddot{y})$, and the coupled equations of motion for the TMDI equipped primary structure in Fig.1 modelled as lumped-mass damped multi degree-of-freedom (MDOF) system are written as

$$\begin{aligned}\left(\mathbf{M}_s(\boldsymbol{\theta}_s) + \mathbf{R}_d m_d \mathbf{R}_d^T + \mathbf{R}_c b \mathbf{R}_c^T\right)\ddot{\mathbf{x}}_s + \left(m_d \mathbf{R}_d + b\mathbf{R}_c\right)\ddot{y} + \mathbf{C}_s(\boldsymbol{\theta}_s)\dot{\mathbf{x}}_s + \mathbf{K}_s(\boldsymbol{\theta}_s)\mathbf{x}_\mathbf{s} \\ = -\left(\mathbf{M}_s(\boldsymbol{\theta}_s) + \mathbf{R}_d m_d \mathbf{R}_d^T\right)\mathbf{R}_s \ddot{x}_g\end{aligned} \tag{2}$$

and

$$(m_d + b)\ddot{y} + \left(m_d \mathbf{R}_d^T + b\mathbf{R}_c^T\right)\ddot{\mathbf{x}}_s + c_d\dot{y} + k_d y = -m_d \mathbf{R}_d^T \mathbf{R}_s \ddot{x}_g\,. \tag{3}$$

In Eq.(2), $\mathbf{M}_s(\boldsymbol{\theta}_s) \in \mathbb{R}^{nxn}$, $\mathbf{C}_s(\boldsymbol{\theta}_s) \in \mathbb{R}^{nxn}$, and $\mathbf{K}_s(\boldsymbol{\theta}_s) \in \mathbb{R}^{nxn}$ are the mass, damping, and stiffness matrices of the primary structure, respectively, where $\boldsymbol{\theta}_s \in \mathbb{R}^{n_{\theta_s}}$ represents the model parameter vector for the structural model. Further, in the previous equations, $\mathbf{R}_s \in \mathbb{R}^n$ is the earthquake influence coefficient vector (vector of ones). Note that in deriving the previous two equations the inerter is taken as weightless, similarly to the spring and to the dashpot, and, therefore, and it does not attract any horizontal seismic inertial force (see also [7,16]). Moreover, Eq. (3) suggests that the total inertia of the TMDI is equal to (m_d+b). The latter observation motivates the definition of the following dimensionless frequency ratio f_d, damping ratio ζ_d, inertance ratio β, and mass ratio μ

$$f_d = \sqrt{\frac{k_d}{(m_d + b)}} / \omega_1 \quad ; \quad \zeta_d = \frac{c_d}{2(m_d + b)\omega_d} \quad ; \quad \beta = b / M \quad ; \quad \mu = m_d / M \tag{4}$$

to characterize the design of the TMDI, where ω_1 and M is the fundamental natural frequency and the total mass of the primary structure.

3 RELIABILITY-BASED DESIGN UNDER STATIONARY STOCHASTIC EXCITATION AND PARAMETRIC UNCERTAINTY

3.1 State-space excitation and structural system modelling

Let $\ddot{x}_g$ in Eqs. (2) and (3) be a stationary filtered Gaussian white noise stochastic process. A state-space formulation is utilized to calculate the response characteristics required in the solution of the optimum TMDI design problem, and in this setting the excitation model is given by

$$\dot{\mathbf{x}}_q(t) = \mathbf{A}_q(\boldsymbol{\theta}_q)\mathbf{x}_q(t) + \mathbf{E}_q w(\mathrm{t}) \quad ; \quad \ddot{x}_g(t) = \mathbf{C}_q(\boldsymbol{\theta}_q)\mathbf{x}_q(t)\,. \tag{5}$$

In the above equation, $w(t) \in \mathbb{R}$ is a zero-mean stationary Gaussian white noise stochastic process with spectral intensity equal to one, $\mathbf{x}_q(t) \in \mathbb{R}^{n_q}$ is the state vector for the excitation, $\mathbf{A}_q(\boldsymbol{\theta}_q) \in \mathbb{R}^{n_q x n_q}$, $\mathbf{E}_q \in \mathbb{R}^{n_q x 1}$ and $\mathbf{C}_q(\boldsymbol{\theta}_q) \in \mathbb{R}^{1 x n_q}$ are the excitation state-space matrices, and $\boldsymbol{\theta}_q \in \mathbb{R}^{n_{\theta_q}}$ collects the parameters used in the analytical definition of the excitation (coloring) filter. Conveniently, the governing equations of motion of the considered structural system in (2) and (3) and the excitation model in (5) can be combined in a single excitation/structural system model in state-space written as

$$\dot{\mathbf{x}}(t) = \mathbf{A}(\boldsymbol{\varphi}, \boldsymbol{\theta})\mathbf{x}(t) + \mathbf{E}w(\mathrm{t}) \quad ; \quad \mathbf{z}(t) = \mathbf{C}(\boldsymbol{\varphi}, \boldsymbol{\theta})\mathbf{x}(t)\,, \tag{6}$$

where $\mathbf{x}(t) \in \mathbb{R}^{n_x}$ is the state vector, with n_x=2n+2+n_q, $\mathbf{z}(t) \in \mathbb{R}^{n_z}$ is the vector of output variables with z_i denoting the i^{th} output component, $\boldsymbol{\theta} = [\boldsymbol{\theta}_s; \boldsymbol{\theta}_q] \subset \mathbb{R}^{n_\theta}$ is the augmented model parameter vector collecting the structural $\boldsymbol{\theta}_s$ and excitation $\boldsymbol{\theta}_q$ model parameters, and $\mathbf{A}(\boldsymbol{\varphi}, \boldsymbol{\theta}) \in \mathbb{R}^{n_x x n_x}$, $\mathbf{E} \in \mathbb{R}^{n_x x 1}$ and $\mathbf{C}(\boldsymbol{\varphi}, \boldsymbol{\theta}) \in \mathbb{R}^{n_z x n_x}$ are the state-space system matrices. Importantly, the matrices $\mathbf{A}$ and $\mathbf{C}$ are functions of both the vectors $\boldsymbol{\varphi}$, collecting the controllable (design) parameters of the TMDI (c_d., k_d, b), and $\boldsymbol{\theta}$. Through proper selection of matrix $\mathbf{C}(\boldsymbol{\varphi},\boldsymbol{\theta})$ the linear model in (6) can be used to

determine the statistics of any response quantity that can be expressed as a linear combination of the state vector **x**. This calculation is briefly summarized next.

3.2 Stationary response statistics

Under the previously discussed excitation modelling assumptions, each output variable z_i $(i=1,...,n_z)$ of the linear dynamic system in (6) given as $z_i = \mathbf{n}_i^T \mathbf{z}$ is a Gaussian stochastic process with zero mean and variance equal to

$$\sigma_{z_i}^2(\boldsymbol{\varphi}\,|\,\boldsymbol{\theta}) = \mathbf{n}_i^T \mathbf{C}(\boldsymbol{\varphi},\boldsymbol{\theta})\mathbf{P}(\boldsymbol{\varphi},\boldsymbol{\theta})\mathbf{C}(\boldsymbol{\varphi},\boldsymbol{\theta})^T \mathbf{n}_i\,, \tag{7}$$

where the state covariance matrix, **P**(**φ**), is determined by solving the Lyapunov equation [17]

$$\mathbf{A}(\boldsymbol{\varphi},\boldsymbol{\theta})\mathbf{P}(\boldsymbol{\varphi},\boldsymbol{\theta}) + \mathbf{P}(\boldsymbol{\varphi},\boldsymbol{\theta})\mathbf{A}(\boldsymbol{\varphi},\boldsymbol{\theta})^T + \mathbf{E}\mathbf{E}^T = 0\,. \tag{8}$$

Further, in evaluating the reliability (i.e., survival probability) of the response quantities z_i required in the optimum TMDI design problem presented in the following sub-section, the variance of the first time derivative of z_i needs to be computed. This is achieved by using the expression

$$\sigma_{\dot{z}_i}^2(\boldsymbol{\varphi}\,|\,\boldsymbol{\theta}) = \mathbf{n}_{z_i}^T \mathbf{C}(\boldsymbol{\varphi},\boldsymbol{\theta})\mathbf{A}(\boldsymbol{\varphi},\boldsymbol{\theta})\mathbf{P}(\boldsymbol{\varphi},\boldsymbol{\theta})\mathbf{A}(\boldsymbol{\varphi},\boldsymbol{\theta})^T \mathbf{C}(\boldsymbol{\varphi},\boldsymbol{\theta})^T \mathbf{n}_{z_i}\,, \tag{9}$$

which is derived under the condition **C**(**φ**,**θ**)**E**=0. The latter is enforced to ensure that the out-crossing rate of the z_i stochastic process discussed in section 3.4 below is finite [11]. Lastly, the transfer function of z_i, also required in the calculation of the out-crossing rate of z_i, is given by

$$H_{z_i}(\omega\,|\,\boldsymbol{\varphi},\boldsymbol{\theta}) = \mathbf{n}_i^T \mathbf{C}(\boldsymbol{\varphi},\boldsymbol{\theta})[i\omega\mathbf{I}_{n_x} - \mathbf{A}(\boldsymbol{\varphi},\boldsymbol{\theta})]^{-1}\mathbf{E}\,, \tag{10}$$

where $i=\sqrt{-1}$ and $\mathbf{I}_u \in \mathbb{R}^{uxu}$ is the identity matrix.

3.3 Reliability-based design formulation with uncertain excitation and structural properties

In this work, reliability related criteria are used to determine the optimum TMDI design variable vector **φ** accounting for uncertainty to the model parameter vector **θ** which contains both excitation and structural properties. Specifically, the design criteria are based on the probability that each output (performance) variable z_i in (6) of interest to seismic design (e.g., inter-storey drift, floor acceleration, etc.) exceeds a given threshold β_i (defining acceptable performance) within some duration T of the excitation (strong ground motion duration). This probability is quantified as

$$P_i(\boldsymbol{\varphi}\,|\,T) = P\Big[\,|z_i(\tau)| > \beta_i \text{ for some } \tau \in [0,T]\,\Big] = \int_{\Theta} P_i(\boldsymbol{\varphi}\,|\,T,\boldsymbol{\theta})\,p(\boldsymbol{\theta})\,d\boldsymbol{\theta} \tag{11}$$

where P[.] stands for probability. In the last equation, p(**θ**) is the probability distribution function (pdf) of the model parameter vector **θ,** describing the relative plausibility of different model parameter values, and Θ corresponds to the region of possible values for **θ** [support of function p(**θ**)]. The above pdf ultimately incorporates the available knowledge expressed in statistical/probabilistic terms about the structural model and the excitation into the design problem. Further, the function $P_i(\boldsymbol{\varphi}\,|\,T,\boldsymbol{\theta})$ is the first-passage probability for output z_i out-crossing the threshold β_i which, in stationary conditions, is approximated by [18]

$$P_i(\boldsymbol{\varphi}\,|\,T,\boldsymbol{\theta}) = 1 - \exp\left(-\nu_i^+(\boldsymbol{\varphi}\,|\,\boldsymbol{\theta})T\right), \tag{12}$$

In the above equation, $\nu_i^+(\boldsymbol{\varphi}\,|\,\boldsymbol{\theta})$ is the conditional out-crossing rate for z_i computed as described in the following sub-section.

From the structural design viewpoint, it is important to note that the quantity $P_i(\boldsymbol{\varphi}\,|\,T)$ in (11) can be interpreted as the probability that the failure mode described by $|z_i| > \beta_i$ occurs. In this regard, the overall design objective function for *robust* design is herein taken as a linear combination of these different probabilities (over all n_z adopted performance variables z_i)

$$J(\boldsymbol{\varphi}) = \sum_{i=1}^{n_z} w_i P_i(\boldsymbol{\varphi} \mid T) = \sum_{i=1}^{n_z} w_i \int_{\Theta} P_i(\boldsymbol{\varphi} \mid T, \boldsymbol{\theta}) p(\boldsymbol{\theta}) d\boldsymbol{\theta} = \int_{\Theta} k(\boldsymbol{\varphi} \mid \boldsymbol{\theta}) p(\boldsymbol{\theta}) d\boldsymbol{\theta} \ , \tag{13}$$

where

$$k(\boldsymbol{\varphi} \mid \boldsymbol{\theta}) = \sum_{i=1}^{n_z} w_i P_i(\boldsymbol{\varphi} \mid T, \boldsymbol{\theta}) = \sum_{i=1}^{n_z} w_i \left[1 - \mathrm{e}^{-\nu_i^+(\boldsymbol{\varphi} \mid \boldsymbol{\theta}) T} \right] \tag{14}$$

and w_i are weighs representing the relative consequences for failure mode $|z_i| > \beta_i$. Therefore, the objective function in (13) considers the contribution of each of the individual failure modes which is aligned with current performance-based earthquake engineering applications [12] that add the contributions from all the examined damage states (failure modes) of interest.

Eventually, the optimal TMDI parameters are obtained through the optimization problem

$$\boldsymbol{\varphi}^* = \arg\min_{\boldsymbol{\varphi} \in \Phi} J(\boldsymbol{\varphi}), \tag{15}$$

where Φ corresponds to the admissible design space. The solution of the robust design problem in (13)-(15) requires the computation of the out-crossing in (12) and the estimation of the multi-dimensional probabilistic integral appearing in the last part of Eq. (13). These two issues are addressed in the following two sub-sections.

3.4 Out-crossing rate calculation

The conditional out-crossing rate for z_i in (12) is given by [18]

$$\nu_i^+(\boldsymbol{\varphi} \mid \boldsymbol{\theta}) = \lambda_i(\boldsymbol{\varphi} \mid \boldsymbol{\theta}) r_i^+(\boldsymbol{\varphi} \mid \boldsymbol{\theta}) \tag{16}$$

and is a product of the Rice's unconditional out-crossing rate $r_i^+(\boldsymbol{\varphi} \mid \boldsymbol{\theta})$ and of the temporal-correlation correction factor $\lambda_i(\boldsymbol{\varphi} \mid \boldsymbol{\theta})$. The first term is given by [19]

$$r_i^+(\boldsymbol{\varphi} \mid \boldsymbol{\theta}) = \frac{\sigma_{\dot{z}_i}(\boldsymbol{\varphi} \mid \boldsymbol{\theta})}{\pi \sigma_{z_i}(\boldsymbol{\varphi} \mid \boldsymbol{\theta})} \exp\left(-\frac{\beta_i^2}{2\sigma_{z_i}^2(\boldsymbol{\varphi} \mid \boldsymbol{\theta})} \right) \tag{17}$$

with the required variances given by (7) and (9). This rate assumes independence between out-crossing events for the process z_i. A temporal correlation factor $\lambda_i(\boldsymbol{\varphi} \mid \boldsymbol{\theta})$ is then utilized to approximately address errors introduced by this independence assumption. This factor is important for problems involving narrow-band systems or cases where out-crossing of threshold β_i is a frequent event and various semi-empirical approximations have been proposed for it. A detailed survey may be found in [18], where it is shown that the choice for the approximation should be based on the bandwidth characteristics of the system. The correction factor proposed by Taflanidis and Beck [18] is herein adopted given by

$$\lambda_i(\boldsymbol{\varphi} \mid \boldsymbol{\theta}) \approx \frac{1 - \exp\left[-q(\boldsymbol{\varphi} \mid \boldsymbol{\theta})^{0.6} \left(\frac{2}{\sqrt{\pi}} \right)^{0.1} \frac{\beta_i \sqrt{2}}{\sigma_{z_i}(\boldsymbol{\varphi} \mid \boldsymbol{\theta})} \right]}{1 - \exp\left[-\frac{\beta_i^2}{2\sigma_{z_i}^2(\boldsymbol{\varphi} \mid \boldsymbol{\theta})} \right]}, \tag{18}$$

where for a process with spectral density $S_{z_i z_i}(\omega \mid \boldsymbol{\varphi}, \boldsymbol{\theta})$

$$q(\boldsymbol{\varphi} \mid \boldsymbol{\theta}) = \frac{\sigma_{z_i}^6(\boldsymbol{\varphi} \mid \boldsymbol{\theta})}{4\pi \int_{-\infty}^{\infty} |\omega| S_{z_i z_i}(\omega \mid \boldsymbol{\varphi}, \boldsymbol{\theta}) d\omega \int_{-\infty}^{\infty} S_{z_i z_i}^2(\omega \mid \boldsymbol{\varphi}, \boldsymbol{\theta}) d\omega}. \tag{19}$$

For the calculation of the integrals in the denominator of Eq. (19), the spectral density $S_{z_i z_i}(\omega|\boldsymbol{\varphi},\boldsymbol{\theta})$ is substituted by the equivalent expression

$$S_{z_i z_i}(\omega|\boldsymbol{\varphi},\boldsymbol{\theta}) = \left|H_{z_i}(\omega|\boldsymbol{\varphi},\boldsymbol{\theta})\right|^2 \tag{20}$$

with $H_{z_i}(\omega|\boldsymbol{\varphi},\boldsymbol{\theta})$ given by Eq. (10). The frequency range over which the dynamics of system are important is partitioned at desired points and the frequency response is calculated. The one-dimensional integral is then evaluated via a standard quadrature rule.

3.5 Estimation of probabilistic integral

Two different approaches are herein discussed for estimation of the integral in (13). The first approach is based on the asymptotic approximation for integrals of this type developed by Papadimitriou et al. [20]. This ultimately entails fitting a scaled Gaussian function over the logarithm of the integrand around its design point, corresponding to the global maximum for it. The original integral is then approximated by the integral corresponding to this fitted function, which leads to the approximate formula

$$J(\boldsymbol{\varphi}) \approx (2\pi)^{n_\theta/2} \frac{k(\boldsymbol{\varphi}|\boldsymbol{\theta}^*)\,p(\boldsymbol{\theta}^*)}{\sqrt{|\mathbf{H}_s(\boldsymbol{\theta}^*|\boldsymbol{\varphi})|}}\ , \tag{21}$$

where $\boldsymbol{\theta}^*$ corresponds to the design point for the integrand

$$\boldsymbol{\theta}^* = \arg\max_{\boldsymbol{\theta}\in\Theta}\left[k(\boldsymbol{\varphi}|\boldsymbol{\theta})\,p(\boldsymbol{\theta})\right]\ , \tag{22}$$

and $\mathbf{H}_s(\boldsymbol{\theta}|\boldsymbol{\varphi}) = \nabla_{\boldsymbol{\theta}}\nabla_{\boldsymbol{\theta}}\left[k(\boldsymbol{\varphi}|\boldsymbol{\theta})\,p(\boldsymbol{\theta})\right]$ is the Hessian of the integrand with respect to $\boldsymbol{\theta}$ which needs to be numerically evaluated. The estimation of Eq. (21) involves small computational effort, especially if dimension of $\boldsymbol{\theta}$ is small (below 5-10 model parameters), but its accuracy is unknown and depends on how well the actual integrand is approximated by the fitted Gaussian. In a number of studies [18, 20-22] this approximation has been demonstrated to yield good accuracy for applications similar to the one examined here.

The second approach for estimation of the integral in (13) is based on stochastic (Monte Carlo) simulation. In this case an unbiased estimate is obtained and the accuracy of that estimate can be controlled by the number of samples utilized [23]. This accuracy can be further increased by using importance sampling (IS). The idea behind IS is to introduce an auxiliary IS density $q(\boldsymbol{\theta})$ so that the computational effort in the stochastic simulation is concentrated in regions of Θ that have higher contribution in the integrand of the probabilistic integral. Using N samples, $\{\boldsymbol{\theta}^j;\ j=1,...,N\}$ from IS density $q(\boldsymbol{\theta})$ the estimate for $J(\boldsymbol{\varphi})$ is

$$J(\boldsymbol{\varphi}) \approx \frac{1}{N}\sum_{i=1}^{N} k(\boldsymbol{\varphi}|\boldsymbol{\theta}^j)\frac{p(\boldsymbol{\theta}^j)}{q(\boldsymbol{\theta}^j)} \tag{23}$$

Even for cases with multiple design points, the estimate in (23) yields a good approximation if $q(\boldsymbol{\theta})$ is chosen such that its peak is near a prominent design point and has as large spread as $p(\boldsymbol{\theta})$ [21].

3.6 Solution of the design optimization problem

For solving the robust design problem an efficient two-stage approach is adopted here. In the first stage the analytic expansion is adopted, leading to the simultaneous optimization for the design points and the optimal design variables

$$\boldsymbol{\theta}^* = \arg\max_{\boldsymbol{\theta}\in\Theta}\left[k(\boldsymbol{\varphi}|\boldsymbol{\theta})\,p(\boldsymbol{\theta})\right] \quad ; \quad \boldsymbol{\varphi}^* = \arg\min_{\boldsymbol{\varphi}\in\Phi}\left[(2\pi)^{n_\theta/2}\frac{k(\boldsymbol{\varphi}|\boldsymbol{\theta}^*)\,p(\boldsymbol{\theta}^*)}{\sqrt{|\mathbf{H}_s(\boldsymbol{\theta}^*|\boldsymbol{\varphi})|}}\right]. \tag{24}$$

Once this stage has converged a refinement of the identified optimum is established using stochastic simulation to calculate the objective function. An IS proposal density is established, $q(\boldsymbol{\theta})$, utilizing the information for the design point $\boldsymbol{\theta}^*$ at the optimal design configuration from the first stage $\boldsymbol{\varphi}^*$. This density then supports the simulation-based optimization

$$\boldsymbol{\varphi}^* = \arg\min_{\boldsymbol{\varphi}\in\Phi} \left[\frac{1}{N} \sum_{i=1}^{N} k(\boldsymbol{\varphi} \mid \boldsymbol{\theta}^j) \frac{p(\boldsymbol{\theta}^j)}{q(\boldsymbol{\theta}^j)} \right] \tag{25}$$

using the previously converged to optimum (stage 1) as an initial point and adopting an exterior sampling approach [24] and a large enough N to facilitate high accuracy estimates (small coefficient of variation). Exterior sampling utilizes the same stream of common random numbers for all design configurations considered within the optimization described by Eq. (25); this creates a consistent estimation error and facilitates significant computational benefits for the numerical optimization. This second stage facilitates ultimately higher accuracy estimates for the objective function and therefore supports a more reliable identification of the optimal design configuration. The higher burden associated within this second stage optimization is reduced by the information utilized by the first stage: a good starting point for the numerical optimization and a IS density that facilitates high accuracy in the vicinity of the optimal solution.

4 ILLUSTRATIVE DESIGN EXAMPLE AND DISCUSSION

The optimal TMDI design approach of section 3 is herein illustrated by considering a particular primary structure and seismic excitation model with parametric uncertainty presented in sub-section 4.1. Selected results from application of the optimal design approach are reported and discussed in sub-section 4.2 for several different values of attached mass and TMDI topologies. Lastly, sub-section 4.3 provides additional data demonstrating the robustness of optimally designed TMDIs to uncertainty in the input and structural parameters.

4.1 Structural and excitation models

A 10-storey lumped mass planar linear shear frame building is adopted as the primary structure with uncertain classical modal damping and uncertain floor stiffnesses involving correlation between different floors. The lumped mass per story is 900ton whereas the nominal stiffness has a gradual decrease along height; it is 782.22MN/m for the bottom four stories, 626.10MN/m for the three intermediate ones and 469.57MN/m for the top three stories. The inter-story stiffnesses k_i of all the stories are parameterized by $k_i = \theta_{ki}\tilde{k}_i$, i=1,..,n, where $\tilde{k}_i$ are the nominal values (mentioned above) and θ_{ki} are non-dimensional uncertain parameters, assumed to be correlated Gaussian variables with mean value one and covariance matrix with elements $\Sigma_{ij}=(0.1)^2\exp[-(i-j)^2/2^2]$. This assumption implies significant correlation between inter-story stiffnesses within two stories apart and a coefficient of variation (c.o.v) of 10%. The damping ratio for all modes ζ is assumed to be a lognormally distributed random variable with median value equal to 0.035% and c.o.v 40%. The natural periods for the nominal structure along with the participation factors in parenthesis are 1.5s (81.7%), 0.55s (11.8%), 0.33s (3.7%).

The stationary seismic excitation $\ddot{x}_g$ is described by a high-pass filtered Kanai-Tajimi power spectrum [25]

$$S_g(\omega) = s_o \frac{\omega_g^4 + 4\zeta_g^2\omega^2\omega_g^2}{\left(\omega_g^2 - \omega^2\right)^2 + 4\zeta_g^2\omega_g^2\omega^2} \frac{\omega^4}{\left(\omega_f^2 - \omega^2\right)^2 + 4\zeta_f^2\omega_f^2\omega^2} \tag{26}$$

In the above equation the Kanai-Tajimi parameters ω_g and ζ_g represent the stiffness/frequency and damping properties, respectively, of the supporting ground modelled by a linear damped SDOF oscillator driven by white noise. Further, the parameters ω_f and ζ_f control the cut-off frequency and

the "steepness" of a high-pass filter used to suppress the low frequency content allowed by the Kanai-Tajimi filter. Lastly, s_o is chosen to achieve a desired pre-specified value for the root mean square acceleration a_{RMS} of the considered seismic input. For the purposes of this study, ω_g, ω_f, ζ_g, ζ_f and a_{RMS} are modeled as lognormal variables with median values 3π, $\pi/2$, 0.4 and 0.8, respectively, and c.o.v 15% for the frequency parameters, 30% for the damping parameters and 5% for a_{RMS}. The duration of excitation T is taken as 15 s. These choices lead to a 5-dimensional $\boldsymbol{\theta}_q$=[ω_g ω_f ζ_g ζ_f a_{RMS}] and a 11 dimensional $\boldsymbol{\theta}_s = [\{\boldsymbol{\theta}_{si}; i = 1,\ldots,10\} \quad \zeta]$.

4.2 Robust reliability-based TMDI design

The structural performance/response variables z_i, i=1,…,n_z considered in the design includes the inter-storey drifts and absolute accelerations for all 10 floors of the adopted primary structure plus the TMD mass displacement (stroke). The corresponding thresholds β_i in (11) are chosen as 3.3 cm for inter-storey drifts, 0.5g for floor accelerations, and 1m for the stroke. Equal weights w_i are assumed in the definition of the design objective function in (13) for all z_i variables. For the uncontrolled (without the TMDI) nominal structure and excitation (median value for all elements of $\boldsymbol{\theta}$ assumed) the objective function (average failure probabilities) is 12.38%. When considering only drift or acceleration responses this value becomes 10.94% and 13.83%, respectively. When uncertainty to the primary structure and excitation is considered the above values become 17.56% (total), 17.43% (drifts) and 17.69% (accelerations).

The vector of dimensionless TMDI design variables is $\boldsymbol{\varphi}=[\zeta_d\ f_d\ \beta]^T$ and includes the damping, frequency and inertance ratios in (4). For the frequency ratio the nominal (median) structural model characteristics are utilized in the definition. The mass ratio μ is treated as a fixed pre-specified variable and a parametric investigation is undertaken for different values of μ ranging from 0.01% to 10%. Furthermore, a set of 8 different TMDI topologies are assessed defined by i_d and i_b floor pairs (i.e., floor numbers where the TMD and the inerter are attached, respectively). Note that, although practical architectural considerations suggest that the inerter would link the m_d mass to the floor immediately above or below the i_d floor, cases in which $|i_d$-$i_b|$=2 are also examined here. Such cases can be facilitated, for example when an atrium exists (e.g., Taipei 101 skyscraper).

Table 1: Optimal performance $J(\boldsymbol{\varphi}^*)$ [%] and optimal inertance ratios in parenthesis for various TMDI topologies defined through i_d, i_b and attached mass ratios.

i_d	i_b	μ (%)									
		0.1	**0.3**	**0.5**	**0.6**	**1**	**1.5**	**3**	**5**	**7**	**10**
10	**9**	10.986 (175.3)	10.883 (172.5)	10.257 (169.5)	9.487$^+$ (0.0)	7.357$^+$ (0.0)	5.810$^+$ (0.0)	3.505$^+$ (0.0)	2.033$^+$ (0.0)	1.269$^+$ (0.0)	0.712$^+$ (0.0)
10	**8**	4.447 (99.9)	4.376 (98.2)	4.308 (97.0)	4.275 (97.2)	4.138 (93.7)	3.977 (90.9)	3.509 (77.2)	2.033$^+$ (0.0)	1.269$^+$ (0.0)	0.712$^+$ (0.0)
9	**8**	5.446 (197.7)	5.403 (195.7)	5.360 (193.8)	5.339 (192.9)	5.255 (188.9)	5.152 (184.0)	4.110$^+$ (0.0)	2.755$^+$ (0.0)	1.977$^+$ (0.0)	1.299$^+$ (0.0)
9	**7**	1.531 (129.3)	1.525 (127.7)	1.518 (126.0)	1.514 (125.5)	1.501 (122.8)	1.484 (119.7)	1.431 (110.9)	1.355 (96.5)	1.256 (72.0)	0.973 (16.9)
8	**7**	3.082 (237.7)	3.073 (235.6)	3.063 (233.6)	3.058 (232.5)	3.039 (228.7)	3.015 (223.8)	2.943 (209.9)	2.845 (190.0)	2.737 (166.1)	2.443$^+$ (0.0)
8	**6**	1.042 (161.2)	1.042 (159.7)	1.042 (158.3)	1.042 (157.8)	1.042 (155.5)	1.042 (152.6)	1.040 (145.4)	1.037 (136.0)	1.029 (125.2)	1.005 (102.1)
7	**6**	3.160 (330.8)	3.153 (329.6)	3.145 (328.5)	3.142 (327.8)	3.127 (325.6)	3.110 (322.9)	3.056 (315.1)	2.988 (304.9)	2.923 (294.4)	2.833 (276.9)
7	**5**	0.849 (185.1)	0.847 (184.8)	0.846 (184.2)	0.846 (184.2)	0.844 (184.0)	0.841 (182.6)	0.834 (180.5)	0.828 (178.0)	0.826 (175.4)	0.826 (170.7)

$^+$ Optimal TMDI design yields a classical TMD (i.e., inertance under optimal design is zero)

In deriving optimal parameters for all the TMDI cases considered, the probabilistic integral in (13) has been transformed to the standard Gaussian space and the two-stage approach discussed in sub-section 3.6 is adopted. For the second stage N=5000 samples are used for the stochastic simulation achieving high accuracy for all cases, with c.o.v less than 2% for most topologies examined. The proposal densities in the second stage are taken as independent Gaussian distributions for each uncertain model parameter with standard deviation equal to 1 and mean equal to the design vector $\boldsymbol{\theta}^*$ identified in the first stage.

Table 1 reports the optimal value of the objective function $J(\boldsymbol{\varphi}^*)$ obtained for all considered TMDI topologies as well as the optimal inertance β and several observations follow. For one, a definite optimum inertance ratio β is obtained in all cases from the optimization approach whose value depends significantly on the mass ratio μ. Above a certain critical mass ratio value, the classical TMD (no inerter included) achieves better performance. In other words, the inclusion of the inerter device is more beneficial for relatively small attached masses, an observation previously reported in the literature in terms of top floor displacement variance minimization [17]. Herein, it is also found that this critical mass ratio value is strongly dependent on the TMDI topology. Examining the structural performance, it is observed that the incorporation of the inerter leads to enhanced vibration suppression compared to the classical TMD. Significantly better performance is achieved for $|i_d\text{-}i_b|$=2 compared to the more conventional $|i_d\text{-}i_b|$=1 cases. Further, for the TMDI cases (non-zero inertance) an increase of the mass ratio does not impact the performance significantly. However, an almost linear positive relationship exists between performance and mass ratio for the TMD cases. Overall, placement of the TMDI at lower floors provides greater efficiency, while for the TMD cases higher floor placement appears to be more beneficial. Lastly, it is generally found that the improvement of performance due to the inclusion of the TMDI is remarkable even for mass ratios as low as 0.1% of the total mass of the structure. As a final remark, it is noted that similar observations and trends have been reported in Giaralis and Taflanidis [9], who considered optimally designed TMDIs through minimizing the probability that any of the considered performance variables z_i (taken same as here) exceeds a given threshold β_i assuming a deterministically known primary structure and seismic excitation frequency content.

4.3 Influence of the structural and excitation model uncertainty to optimal TMDI design

As a measure of the achieved robustness of the TMDI vis-à-vis the classical TMD, the sensitivity of the optimum reliability-based performance achieved to uncertainties in the structural and excitation models is examined. This sensitivity is quantified through the ratio of optimal performance for the nominal case (i.e., design for deterministically known primary structure and excitation) $J(\boldsymbol{\varphi}_n^*)$ over the optimal performance under uncertainty reported in Table 1. Table 2 reports this ratio, $J(\boldsymbol{\varphi}_n^*)/J(\boldsymbol{\varphi}^*)$, for all TMDI topologies and attached masses considered before.

Table 2: Performance under uncertainty if the nominal design was adopted to the corresponding optimal performance $J(\boldsymbol{\varphi}_n^*)/J(\boldsymbol{\varphi}^*)$.

i_d	i_b	μ (%)											
		0.1	**0.3**	**0.5**	**0.6**	**0.75**	**1**	**1.5**	**2**	**3**	**5**	**7**	**10**
10	**9**	1.01	1.01	1.02	1.02$^+$	1.01$^+$	1.01$^+$	1.02$^+$	1.04$^+$	1.08$^+$	1.42$^+$	1.45$^+$	1.20$^+$
10	**8**	1.01	1.01	1.01	1.01	1.01	1.01	1.01	1.01	1.02	1.42$^+$	1.45$^+$	1.20$^+$
9	**8**	1.00	1.00	1.00	1.00	1.00	1.00	1.00	1.00	1.08$^+$	1.04$^+$	1.06$^+$	1.11$^+$
9	**7**	1.00	1.00	1.00	1.00	1.00	1.00	1.00	1.00	1.00	1.00	1.00	1.06
8	**9**	1.00	1.00	1.00	1.00	1.00	1.00	1.01	0.91	1.00	1.03$^+$	1.04$^+$	1.05$^+$
8	**6**	1.01	1.01	1.01	1.01	1.01	1.01	1.01	1.01	1.02	1.02	1.02	1.01
7	**6**	1.00	1.00	1.00	1.00	1.00	1.00	1.00	1.00	1.00	1.00	1.00	1.01
7	**5**	1.01	1.01	1.01	1.01	1.01	1.01	1.01	1.00	1.00	1.00	1.00	1.00

$^+$ Optimal TMDI design yields a classical TMD (i.e., inertance under optimal design is zero)

These results clearly indicate that the TMDI enjoys a very high degree of robustness with respect to structural and excitation uncertainties; the performance $J(\boldsymbol{\varphi}_n^*)$ is very similar to $J(\boldsymbol{\varphi}^*)$ in all studied topologies. However, this is not the case for the TMD for which the ratio $J(\boldsymbol{\varphi}_n^*)/J(\boldsymbol{\varphi}^*)$ is consistently higher than one. This observation can be attributed to detuning effects for the TMD which do not seem to affect the TMDI. This assertion is reinforced by the fact that for the largest value of the attached mass considered (μ=10%) and for the commonly used TMD topology (mass attached to the top floor), an increased robustness is attained compared to the μ=7% and μ=5% cases, while it is well-known that large-mass TMDs are more robust to detuning effects (e.g. Hoang et al.).

5 CONCLUDING REMARKS

A first-passage reliability based approach was considered for the optimum design of the recently proposed TMDI to control the dynamic response of linear building frames subject to stationary seismic excitations and accounting for parametric structural and excitation uncertainty. Different failure modes were examined for defining acceptable performance, extending to inter-storey drifts and floor acceleration responses for the primary structure as well as displacement responses of the attached mass. The design variables included the inertance (mass amplification property) of the inerter as well as the TMDI linear spring and damping constants. The illustrative example demonstrated the enhanced performance of the TMDI over the classical TMD especially for relatively small additional attached mass. More importantly, it was shown that the TMDI is significantly more robust to the considered uncertainties than the classical TMD, even compared to TMDs with an order of magnitude larger attached mass. Future work will include treating the mass ratio as a design parameter as well as the consideration of TMDI topology optimization. Further, robust to uncertainty optimization techniques accounting for the non-stationary nature of the seismic excitation as well as the potential non-linear behaviour of the primary structure due to yielding will also be considered.

ACKNOWLEDGEMENTS

The first author gratefully acknowledges the financial support of EPSRC in UK under grant EP/M017621/1.

REFERENCES

[1] Rana, R. & Soong, T.T. Parametric study and simplified design of tuned mass dampers, *Engineering Structures*, 1998; **20**:193-204.

[2] Hoang, N., Fujino, Y. & Warnitchai, P. Optimal tuned mass damper for seismic applications and practical design formulas, *Engineering Structures*, 2008; **30**:707-715.

[3] Moutinho, C. An alternative methodology for designing tuned mass dampers to reduce seismic vibrations in building structures, *Earthquake Engineering & Structural Dynamics*, 2012; **41**: 2059-2073.

[4] De Angelis, M., S. Perno, and A. Reggio, Dynamic response and optimal design of structures with large mass ratio TMD. *Earthquake Engineering & Structural Dynamics*, 2012; **41**:41-60.

[5] Tigli, O.F. Optimum vibration absorber (tuned mass damper) design for linear damped systems subjected to random loads, *Journal of Sound and Vibration*, 2012; **331**:3035-3049.

[6] Marian, L. & Giaralis, A. Optimal design of inerter devices combined with TMDs for vibration control of buildings exposed to stochastic seismic excitations, In: *11th International Conference on Structural Safety and Reliability* (ICOSSAR, June 16-20, 2013, NY), paper #137, 1025-1032.

[7] Marian, L. & Giaralis, A. Optimal design of a novel tuned mass-damper-inerter (TMDI) passive vibration control configuration for stochastically support-excited structural systems. *Probabilistic Engineering Mechanics*, 2014; **38**:156-164.

[8] Smith, M.C. Synthesis of mechanical networks: The Inerter, *IEEE Transactions in Automatic Control*, 2002; 47:1648-1662.

[9] Giaralis, A. & Taflanidis AA. (2015). Reliability-based design of tuned-mass-damper-inerter (TMDI) equipped stochastically support excited structures. In: *Proceedings of the 12th International Conference on Applications of Statistics and Probability in Civil Engineering*- (ICASP12, July 12-15, 2015, Vancouver, Canada), p.10.

[10] Giaralis, A. & Marian, L. (2016). Use of inerter devices for weight reduction of tuned mass-dampers for seismic protection of multi-story building: the Tuned Mass-Damper-Interter (TMDI), *Proceedings SPIE 9799, Active and Passive Smart Structures and Integrated Systems 2016*, 97991G (April 15, 2016); doi:10.1117/12.2219324.

[11] Taflanidis, A. A. & Scruggs, J. T. Performance measures and optimal design of linear structural systems under stochastic stationary excitation, *Structural Safety*, 2010; **32**:305-315.

[12] Goulet, C.A., Haselton, C.B., Mitrani-Reiser, J., Beck, J.L., Deierlein, G., Porter, K.A. & Stewart, J.P. Evaluation of the seismic performance of code-conforming reinforced-concrete frame building-From seismic hazard to collapse safety and economic losses. *Earthquake Engineering and Structural Dynamics*, 2007; **36**:1973-1997.

[13] Papageorgiou, C. & Smith, M.C. Laboratory experimental testing of inerters, *IEEE Conference on Decision and Control*, 2005;**44**:3351-3356.

[14] Wang, F.C., Hong, M.F. & Lin, T.C. Designing and testing a hydraulic inerter, *Journal of Mechanical Engineering Science,* 2011;**225**:66-72.

[15] Swift, S.J., Smith, M.C., Glover, A.R., Papageorgiou, C, Gartner, B. & Houghton, N.E. Design and modelling of a fluid inerter," *International Journal of Control*, 2013; **86**:2035-2051.

[16] Takewaki, I., Murakami, S., Yoshitomi, S. & Tsuji, M. Fundamental mechanism of earthquake response reduction in building structures with inertial dampers, *Structural Control and Health Monitoring*, 2012;**19**:590-608.

[17] Lutes, L. D. & Sarkani, S. *Stochastic analysis of structural and mechanical vibrations*, Prentice Hall, Upper Saddle River, New Jersey, 1997.

[18] Taflanidis, A.A. and J.L. Beck, Analytical approximation for stationary reliability of certain and uncertain linear dynamic systems with higher dimensional output. *Earthquake Engineering and Structural Dynamics*, 2006. **35**(10): p. 1247-1267.

[19] Rice, S. O. Mathematical analysis of random noise, *Bell System Technical Journal*, 1944/45, **23/24**.

[20] Papadimitriou, C., J. Beck, and L. Katafygiotis, Asymptotic expansions for reliabilities and moments of uncertain dynamic systems. *Journal of Engineering Mechanics*, 1997. **123**: p. 1219-1229.

[21] Au, S.K., C. Papadimitriou, and J.L. Beck, Reliability of uncertain dynamical systems with multiple design points. *Structural Safety*, 1999. **21**: p. 113-133.

[22] Taflanidis, A.A., Reliability-based optimal design of linear dynamical systems under stochastic stationary excitation and model uncertainty. *Engineering Structures*, 2010. **32**(5): p. 1446-1458.

[23] Robert, C.P. & G. Casella, *Monte Carlo Statistical Methods*. 2nd ed. Springer, New York, 2004.

[24] Spall, J.C., *Introduction to stochastic search and optimization*. Wiley-Interscience, New York, 2003.

[25] Clough, R. W. & Penzien, J. *Dynamics of structures*, McGraw-Hill Inc., New York, 1993.